

# Pipe effect in viscous liquids

V. Capano

*Dipartimento di Scienze Fisiche, Università di Napoli “Federico II”,  
Complesso Universitario di Monte S. Angelo, via Cinthia, I-80126 Naples, Italy*

S. Esposito\*

*Dipartimento di Scienze Fisiche, Università di Napoli “Federico II”  
and Istituto Nazionale di Fisica Nucleare, Sezione di Napoli,  
Complesso Universitario di Monte S. Angelo, via Cinthia, I-80126 Naples, Italy*

G. Salesi†

*Università Statale di Bergamo, Facoltà di Ingegneria, viale Marconi 5, I-24044 Dalmine (BG), Italy  
and Istituto Nazionale di Fisica Nucleare, Sezione di Milano, via Celoria 16, I-20133 Milan, Italy*

A detailed experimental and theoretical study has been performed about a phenomenon, not previously reported in the literature, occurring in highly viscous liquids: the formation of a definite pipe structure induced by the passage of a heavy body, this structure lasting for quite a long time. A very rich phenomenology (including mechanical, optical and structural effects) associated with the formation of the pipe has been observed in different liquids. Actually, the peculiar dynamical evolution of that structure does not appear as a trivial manifestation of standard relaxation or spurious effects. In particular we have revealed different time scales during the evolution of the pipe and a non-monotonous decreasing of the persistence time with decreasing viscosity (with the appearance of at least two different maxima). A microscopic model consistent with the experimental data, where the pipe behaves as a cylindrical dielectric shell, has been proposed. The general time evolution of the structure has been described in terms of a simple thermodynamical model, predicting several peculiarities effectively observed.

PACS numbers: 64.70.Dv, 64.70.Ja, 64.60.My, 36.40.-c, 77.22.-d

## I. INTRODUCTION

One of the most active area of research in soft condensed matter physics, physical chemistry, materials science and biophysics is the study of the dynamics of complex systems and their relationship to the structure. Among such complex systems, a special place is occupied by hydrogen-bonding liquids and their mixtures [1] [2], due to their extreme prominence in different biological and technological processes. This is especially true for glycerol ( $C_3H_8O_3$ ), for which the presence of three hydroxyl groups per molecule makes it a particularly rich and complex system for the study of hydrogen bonded fluids. Glycerol, indeed, has been the subject of considerable and long-standing scientific interest [3] due to its complex nature.

For example, the peculiarities of the intermolecular interaction of glycerol with water via hydrogen bonds form the basis of the valuable hydration properties of glycerol, that are widely applied in the pharmaceutical, cosmetics and food industries. Just to quote typical examples, glycerol has been employed as a cryoprotector [4], depending upon the changes of the parameters of the phase transitions of water in the presence of glycerol, but it has been

also the focus of study by researchers in cryopreservation [5].

On the other hand, glycerol is an excellent glass former, and has been extensively studied experimentally [6] in connection with attempts to understand the nature of the glass transition. Understanding the liquid-glass transition and its related dynamics, in fact, is one of the most important and challenging problems in modern condensed matter physics, and glycerol and its mixtures with water are widely used as models to study the cooperative dynamics, glass transition phenomena and scaling properties in complex liquids.

The dielectric properties of hydrogen-bonded liquids are, as well, of key interest, because such liquids generally shows abnormal dielectric behavior, which is not observed in a non-hydrogen-bonded liquid. In fact, with some exception (such as acetic acid), the static dielectric constant of a hydrogen-bonded liquid is generally larger than that of a normal polar one, mainly because of the regular alignment of a dipolar molecule in the hydrogen-bonded cluster. This applies especially to glycerol, where the existence of long- and short-ranged forces, and a large variety of possible molecular conformations, leads to important dynamics on a variety of time scales.

All these facts evidently motivate, on one hand, the large research effort about hydrogen-bonded liquids and, in particular, glycerol, but also urge to study further such systems, searching for possible novel phenomena that put some other light on their interesting physical properties.

---

\*Electronic address: Salvatore.Esposito@na.infn.it

†Electronic address: Giovanni.Salesi@unibg.it

In the present paper we extensively report just on an apparently new effect of such kind observed in glycerol that, seemingly, has not been considered before (at least in the published literature).

The starting observation is strictly related to the standard determination of the viscosity by means of the method of the falling sphere. Although not easily seen with the naked eye, after the falling of the metal sphere in glycerol at common temperatures, a pipe appears in the viscous liquid that persist for some long time. At a first glance, such a not surprising effect seems to be easily explained in terms of some relaxation processes occurring in highly viscous media. However, the lacking of an apparent microscopic structure in liquids, though highly viscous, similar to solids seems mainly to disfavor the simple explanation envisaged above, while requiring more observations on the phenomenon. Indeed, such observations do reveal a very rich phenomenology, pointing out that the effect observed is, quite surprisingly, not at all trivial.

We have thus started a set of appropriate experiments aimed at collecting all the relevant phenomenology (both qualitative and quantitative), upon which a theoretical explanation of the phenomenon, though preliminary, may be consistently built. The results of our large study are reported here. After a detailed description in Sections II of all the experimental observations obtained, together with the report on the results of data fitting and their interpretation, in Section III we give possible theoretical interpretation of the phenomena observed. In particular, we propose a possible microscopic interpretation of the occurrence of the pipe effect, discussing quite in detail the corresponding theoretical model, and discuss and solve a thorough thermodynamical model describing the evolution of the pipe, deducing some of the properties observed. Finally, in Section IV, we summarize the results obtained and give our conclusions and outlook.

## II. PHENOMENOLOGY

In the experiments performed, we have employed different commercial viscous liquids, glycerol ( $C_3H_8O_3 \geq 99.5\%$ , water content  $\leq 0.1\%$ ), ethanol ( $C_2H_6O \geq 96\%$ ) and castor oil (essentially pure), as delivered, while, for the mixtures with water, a doubly distilled water was used. We have focused our attention particularly to glycerol, whose main physical properties (and, for comparison, those of water) are reported in Table I for a reference temperature. For practical and interpretational uses, it is also helpful to take into account the dependence of the most directly relevant properties of the viscous liquids used on temperature  $T$  (always given in Celsius degrees  $^{\circ}C$ ) and concentration  $x$ ; the corresponding graphs are showed in Figures 1, 2. For the sake of simplicity, in the following we will refer to “pure” glycerol when no solute (water or ethanol) has been added; we have checked that, in such case, the concentration of glycerol is about

	Property	Glycerol	Water
$M$	Molecular weight (g/mol)	92.09	18.01
$\rho$	Density <sup>a</sup> (Kg/m <sup>3</sup> )	1258.02	997.05
$\eta$	Viscosity <sup>b</sup> ( $10^{-3}$ Pa·s)	1410	1.0016
$\sigma$	Surface tension <sup>c</sup> ( $10^{-3}$ N/m)	64.00	71.98
$\beta$	Compressibility, isothermal ( $10^{-10}$ /Pa)	$1 \div 0.1^d$	$4.599^c$
$c$	Specific heat <sup>a</sup> (J/Kg·°K)	$2406 \div 2425$	4181.9
$\kappa$	Thermal conductivity <sup>c</sup> (W/m·°K)	0.285	0.610
$\gamma$	Thermal expansion coefficient <sup>c</sup> ( $10^{-6}$ /°K)	615	253
$\mu$	Electric dipole moment ( $D = 3.33564 \cdot 10^{-30}$ C·m)	$2.68^e$	$2.95^f$
$\alpha$	Polarizability volume ( $10^{-30}$ m <sup>3</sup> )	8.13	1.470
$\varepsilon$	Dielectric constant <sup>c</sup>	40.10	78.4
$n$	Refractive index <sup>g</sup>	1.47399	1.33286

<sup>a</sup>At 25°C, 101.325kPa.

<sup>b</sup>At 20°C, 101.325kPa.

<sup>c</sup>At 25°C.

<sup>d</sup>See L.J. Root and B.J. Berne, J. Chem. Phys. **107** (1997) 4350.

<sup>e</sup>See K.D. Cook, P.J. Todd and D.H. Friar, Biomed. Environ. Mass Spectrom. **18** (1989) 492.

<sup>f</sup>At 27°C

<sup>g</sup>At 25°C,  $\lambda = 589.26$ nm

TABLE I: Main physical properties of liquid glycerol [7] and water [8].

$x = 0.99$  (mainly due to pre-existing impurities), that will then be our reference value.

The several experiments carried out consisted, basically, always in inducing the formation of the pipe in the viscous liquid, just by means of the falling (from the rest) of steel spheres of different diameters, and then observing various properties about the formation and evolution of the pipe, or measuring different properties of the pipe itself. For obvious reasons, we have taken some care in keeping constant and uniform the relevant parameters (pressure, temperature, concentration, etc.) of the probing liquids, contained in given graduated tubes (heights ranging from 15 to 30 cm, diameters from 2 to 5 cm).

While the formation of the pipe follows closely the falling of the sphere (it, is, practically, instantaneous), its disappearance after some time is not, in the given experimental conditions, unambiguous. In order to keep the errors on the persistence time of the phenomenon under control, we have always adopted the same protocol to mark the “complete” disappearance of the pipe (that is, when the luminosity of the pipe with respect to the bulk liquid falls below a given value, necessarily different from zero).

For the study of the optical properties of the pipe, we have used standard filament and halogen lamps, and a common He-Ne laser.

The properties of the pipe have been studied in four different kinds of viscous liquids, namely: pure glycerol, glycerol/water mixtures and glycerol/ethanol mixtures

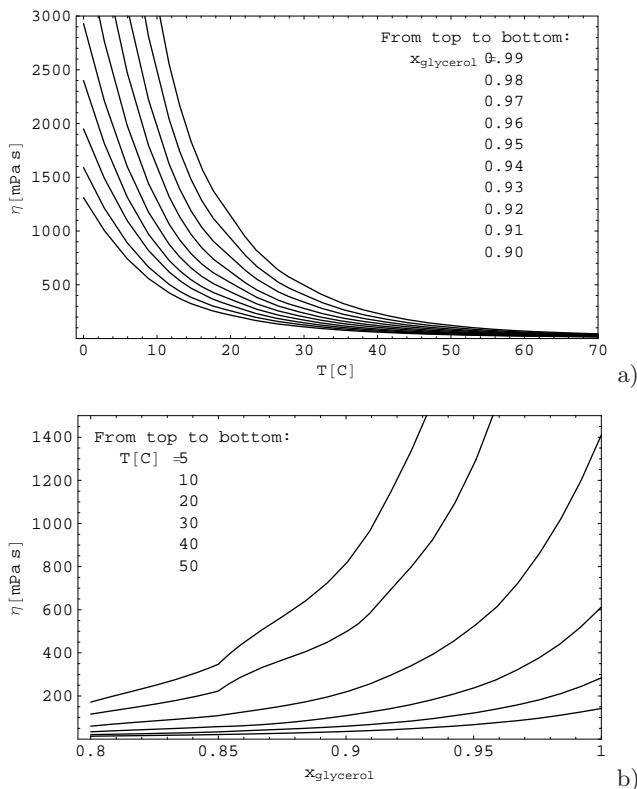


FIG. 1: Dependence of the viscosity  $\eta$  of glycerol-water solutions on (a) temperature  $T$ , and (b) concentration  $x_{\text{glycerol}}$  of glycerol.

[The curves have been elaborated from numerical data given by “The Dow Chemical Company” on the website <http://www.dow.com/glycerine/resources/physicalprop.htm>.]

with different concentrations, and pure castor oil. The motivation for this choices lies in their structural properties and, in particular, on the values of two main quantities of those substances, that are viscosity and surface tension. Indeed, glycerol has very high viscosity ( $\eta_{\text{glycerol}} = 1410 \times 10^{-3} \text{ Pa} \cdot \text{s}$  at  $20^\circ\text{C}$ ) and surface tension ( $\sigma_{\text{glycerol}} = 63.4 \times 10^{-3} \text{ N/m}$  at  $20^\circ\text{C}$ ), while water and ethanol have a low viscosity ( $\eta_{\text{water}} = 1.002 \times 10^{-3} \text{ Pa} \cdot \text{s}$  and  $\eta_{\text{ethanol}} = 1.200 \times 10^{-3} \text{ Pa} \cdot \text{s}$  at  $20^\circ\text{C}$ ) but high ( $\sigma_{\text{water}} = 72.8 \times 10^{-3} \text{ N/m}$  at  $20^\circ\text{C}$ ) and intermediate ( $\sigma_{\text{ethanol}} = 22.8 \times 10^{-3} \text{ N/m}$  at  $20^\circ\text{C}$ ) surface tension, respectively, so that, with different mixtures, at least the dependence on viscosity and surface tension of pipe formation and evolution may be discriminated. The use, in further experiments, of castor oil too, which have an high viscosity, comparable to that of pure glycerol ( $\eta_{\text{castoroil}} = 986 \times 10^{-3} \text{ Pa} \cdot \text{s}$ ), but a completely different molecular structure, may shed some light on the influence of the structure on the phenomenon.

In the following we will report schematically the different observations obtained, appropriately grouped on the basis of their physical content.

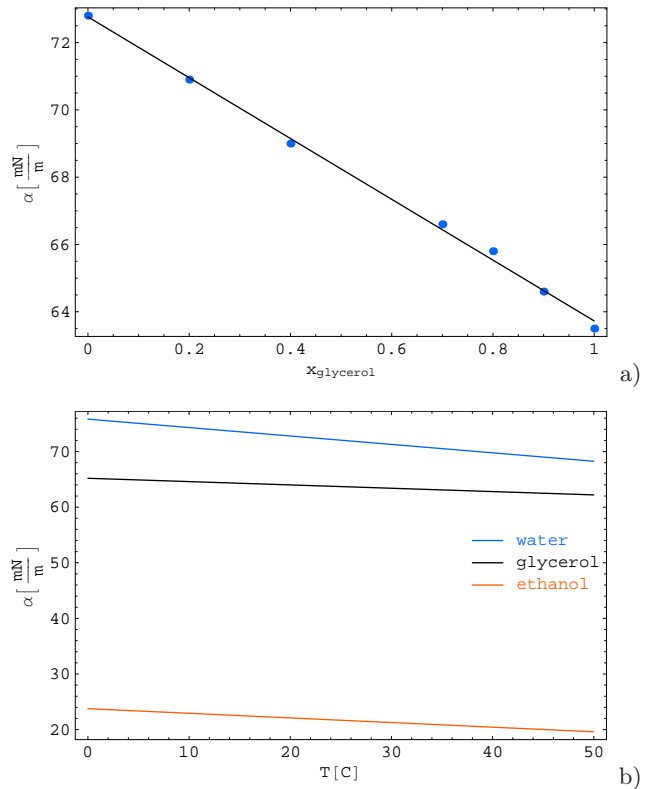


FIG. 2: a) Dependence of the surface tension  $\sigma$  of glycerol-water solutions on the concentration  $x_{\text{glycerol}}$  of glycerol ( $T = 20^\circ\text{C}$ ). The data are approximated by the relation  $\sigma = 72.76 - 9.04x_{\text{glycerol}}$ .

[Elaboration on the numerical data given by N.R. Morrow, “Fundamentals of reservoir surface energy as related to surface properties, wettability, capillary action, and oil recovery from fractured reservoirs by spontaneous imbibition”, Quarterly Report DE-FC26-03NT15408, from the U.S. DOE’s Office of Scientific and Technical Information website <http://www.osti.gov>.]

b) Dependence of the surface tension  $\sigma$  of pure liquids (water, glycerol and ethanol) on the temperature  $T$ . The curves correspond to the following fitting relations:  $\sigma_{\text{water}} = 72.8 - 0.1514(T - 20)$ ,  $\sigma_{\text{glycerol}} = 64.0 - 0.0598(T - 20)$ ,  $\sigma_{\text{ethanol}} = 22.1 - 0.0832(T - 20)$ .

[Elaboration on the numerical data reported on the website <http://www.surface-tension.de> della DataPhysics Instruments.]

## A. Qualitative observations

### 1. Pipe formation

F1. The pipe is generated after the falling of spheres of different diameters in pure glycerol, irrespective of the starting falling conditions (from outside the tube or from inside the glycerol), the diameters (from 2 mm to 12 mm) and the shape (cylinder or prism with different basis) of the tubes.

F2. The pipe does not form (in any kind of tubes, in vertical or inclined positions) if, before falling, the

spheres are deposited in pure glycerol for a very long time (greater than five hours).

F3. The pipe does not form if, instead of falling steel spheres, a (macroscopic) air bubble is used during its reclimbing motion in pure glycerol.

F4. The pipe is generated (in a very visible way) if, instead of falling steel spheres, water droplets on the bottom of the tube are used in their reclimbing motion in pure glycerol. The pipe, however, deforms very rapidly (water is soluble in glycerol) and, after a given time, all the water is absorbed by glycerol, leaving no track of its passage.

F5. The pipe is generated even in non-pure glycerol, that is in glycerol/water mixtures (with concentration as low as  $x_{\text{glycerol}} = 0.80$ ) and in glycerol/ethanol mixtures[14] (with concentration as low as  $x_{\text{glycerol}} = 0.90$ ).

F6. When observing the projection (see the point O4) of the pipe generated in glycerol/water mixtures with an high concentration of water (around 8% in weight of water), just after the falling of the sphere the pipe appears to be not homogeneous but as formed by alternatively bright and dark vertical strips. The passage of the reclimbing mass, considered at point S3, compact such strips and the pipe becomes homogeneous.

F7. The pipe generated in glycerol/ethanol mixtures, for any concentration considered, appears (see the point O1) to have a more pronounced cylindrical structure with respect to its formation in pure glycerol or in glycerol/water mixtures (the pipe appears, effectively, as a “tube immersed” in the bulk liquid).

F8. The pipe is generated by falling spheres even in castor oil, although in a less marked way.

## 2. Dynamics of pipe formation

D1. Just after the falling of the sphere in pure glycerol, the diameter of the pipe generated coincides with that of the sphere but, very rapidly, the pipe grows thinner till its diameter takes a stationary value (largely lower than the diameter of the sphere). Such a thinning takes place by means of liquid reclimbing around the pipe towards the top of the tube rather than by means of a narrowing/absorption process. (see also the point S3.)

D2. Just after the falling of spheres with large diameters (around 10 mm), a double pipe structure is observed: a pipe with lower diameter is inside a larger pipe.[15] Quite rapidly, however, the outer pipe gets narrower till it coincides with the inner one.

D3. For a sphere put at rest in pure glycerol for a not extremely large time (up to 4-5 hours), that is allowed to fall along one side of an inclined parallelepiped (small inclinations), the glycerol flow gliding from the front to the back of the falling sphere is observed[16], the flow closing behind the sphere. In such a case, the pipe is not perceptible (see also the point F2).

D4. In the same conditions of point D3, but putting

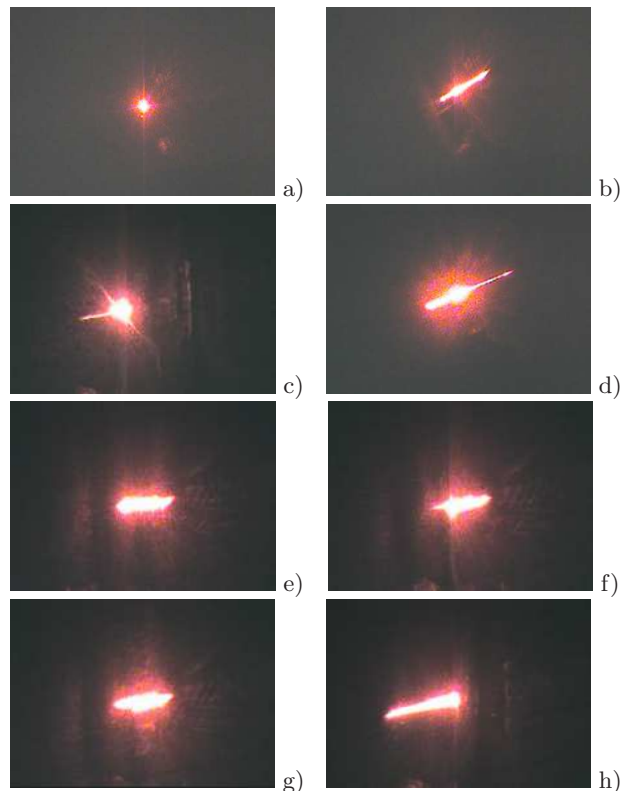


FIG. 3: Scattering of a laser beam from a pipe generated in glycerol (O8 effect, see the text).

the sphere at rest in glycerol for extremely long times (about one day), the glycerol flow is barely perceptible, while for longer times it is completely unobservable. In any case, a pipe is not generated (see also the point F2).

## 3. Size and shape of the pipe

G1. The upper part of the pipe (in pure glycerol) is funnel-shaped, while rapidly narrowing to a cylinder towards the bottom.

G2. The sizes of pipes generated by differently sized spheres are not proportional to the diameters of the spheres. For example, by doubling the diameter of a falling sphere, the pipe generated is only slightly larger.

G3. In glycerol/water and glycerol/ethanol mixtures, the shape of the pipe is not regularly cylindrical (with a definite straight line axis) as in the case of pure glycerol.

G4. For a given sized sphere, the pipe generated in castor oil has a smaller diameter with respect to that generated in glycerol (or glycerol mixtures).

## 4. Pipe evolution

E1. The persistence time (time from the formation of the pipe till its disappearance) depends on the concentration of glycerol, when glycerol/water and glyce-



erol/ethanol mixtures are used: by lowering the concentration of glycerol, the persistence time gets shorter (see quantitative results below).

E2. Before the pipe disappears, it gets deformed (its shape is no more cylindrical with a straight line axis), such a deformation apparently depending on the (horizontal and vertical) sizes of the tubes employed.

E3. Before the pipe disappearance, its deformation in glycerol/water and glycerol/ethanol mixtures is analogous to that in pure glycerol, but more accentuated (for lower glycerol concentrations).

E4. The persistence time of the pipe generated in castor oil is much shorted with respect to (pure or mixed) glycerol (see quantitative results below).

### 5. Mechanical effects

M1. A mechanical action may be performed upon the pipes generated in pure glycerol without breaking them (they can be shifted, winded one around another, and so on).

M2. During the reclimbing motion of a (macroscopic) air bubble generated at the bottom of a pipe with diameter lower than that of the bubble, the pipe widens out, taking again its original shape after the passage of the bubble.

M3. The pipe generated in pure glycerol may be mechanically deformed, generating novel pipes through bifurcations. In particular, it is possible to “close” the pipe by “transporting” backward (that is, in the direction opposite to that of formation)) its surface. In such a case, however, although the pipe is re-absorbed, a perturbed crater-like zone persists (for some time) on the free surface of glycerol.

### 6. Optical effects

O1. The pipe is visible only along its axis (from the top), but not at its sides.

O2. The pipe generated in castor oil is less visible from the top with respect to glycerol and glycerol mixtures.

O3. The pipe generated in pure glycerol becomes more glossy than the bulk glycerol if illuminated along its axis (from the top) with normal (not laser) light.

O4. The pipe generated in pure glycerol produces a shadow (with respect to the bulk glycerol) on a screen when illuminated at its sides with normal light of not extremely high intensity. (For very high light intensities, both the pipe and the bulk glycerol appear on the screen with practically the same luminosity, so that it is hard to discriminate among them.)

O5. The projection of the pipe (illuminated at its sides) on a screen shows a greater luminosity (with respect to the bulk glycerol) at the pipe surface, while its internal part is dark, even with respect to the bulk glycerol. This can be observed when the light impinges per-

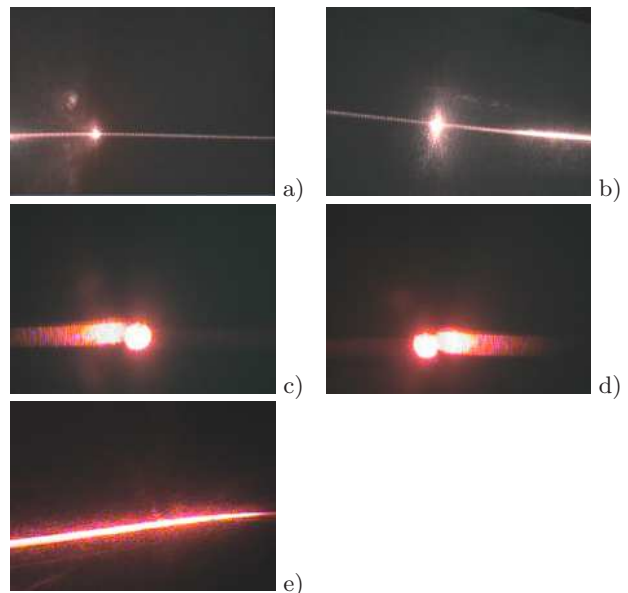


FIG. 4: Scattering of a laser beam from a glass tube immersed in glycerol and filled with (a,b) water or (c,d) glycerol (O8 effect, see the text). In e): particular of the scattered beam (tube filled with water or glycerol).

pendicularly both on the tube and on the pipe surface. By increasing the angle of incidence, the brighter edges increase in width “invading” the dark internal part, till they completely cover the internal part. In such a case, all the projection of the pipe is brighter with respect to the bulk glycerol.

O6. The projection of the pipe generated in castor oil is barely visible on a screen, when illuminated at its sides with normal light, since its “shadow” on the screen is slightly brighter than the bulk liquid.

O7. The bright/dark effect effect of the point O5, including its dependence on the angle of incidence, is not observed in the pipes formed in castor oil.

O8. A laser beam (of sufficiently high intensity), impinging on a pipe generated in glycerol, is scattered normally to the pipe surface, the light disc on the screen becoming elliptical in its shape (see Fig. 3). Such scattering is similar to that from a glass (or plastic) tube filled with a fluid (air, water or glycerol) and immersed into a tube filled with glycerol, but remarkable differences arises (see Fig. 4). Indeed, in such an “ideal” case the light disc is scattered to form a segment which is very thin and long, and extends to both parts of the glass tube when the laser beam impinges tangentially on it. Instead, for non-tangential incidence, the scattered beam results largely deviated on the screen, the deviation being smaller when filled with glycerol, while greater when filled with water or air.

O9. When the pipe generated in glycerol is not regularly (cylindrical) shaped, or some inhomogeneities are present near its surface, the laser beam scattered from

such surface presents (apart from its long and narrow form discussed above) bright fringes alternated with dark ones. These are visible for any angle of incidence, even when the laser impinges on the backward lateral surface of the pipe (see Fig. 5).

O10. The O8 effect is observed even for pipes generated in glycerol/water mixtures, with similar results.

O11. The O8 effect is not observed in pipes generated in castor oil.

### 7. Secondary effects

S1. If the steel sphere is left to fall in the glycerol starting from a point outside it (i.e., in air), microscopic air bubbles are present in the pipe along its full length. Such micro-bubbles climb up very slow (they are, practically, trapped inside the pipe), and render much more visible the pipe when illuminated.

S2. The trapping of air micro-bubbles (S1 effect) is present even in the pipe generated in castor oil, but the micro-bubbles are more scattered among them (or less concentrated) with respect to glycerol.

S3. After some time (parting time) from pipe formation, a fluid mass parts from the sphere boundary at the bottom of the pipe formed in glycerol/water mixtures, such mass being previously “glued” (due to its high viscosity and surface tension) to the sphere. The fluid mass climbs up very slowly along the pipe, this widening out and taking again its original shape after the passage of the mass (as in the M2 effect).

S4. For a given diameter of the steel sphere, the parting time of the S3 effect depends on the water concentration of the mixture, the time being smaller for a greater content of water.

S5. For a given water concentration of the mixture, the parting time of the S3 effect depends on the diameter of the generating sphere, the time being smaller for smaller diameters.

### 8. Density and viscosity of the pipe

P1. The pipes generated in pure glycerol not in a vertical position, but anyhow inclined, slowly climb up in the bulk glycerol. This unambiguously shows that the density of the fluid inside the pipe is slightly lower than that of the bulk glycerol.

P2. In any working condition, the terminal velocity of spheres falling inside a pipe is slightly greater than that of spheres falling in the bulk glycerol. This unambiguously shows that the viscosity of the fluid inside the pipe is slightly lower than that of the bulk glycerol.

Although quite unfavorable experimental conditions have prevented us to be accurate in the determination of the density and the viscosity of the pipe liquid, nevertheless we have established that the per cent variation of

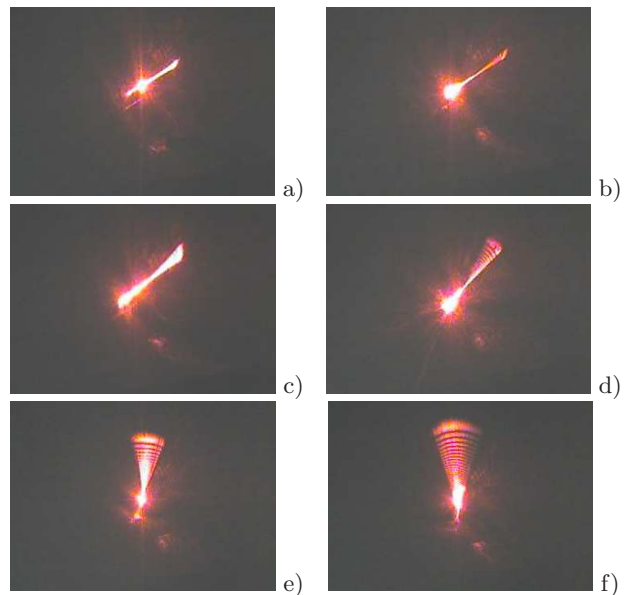


FIG. 5: Scattering of a laser beam from an inhomogeneous surface of a pipe generated in glycerol (O9 effect, see the text).

such physical quantities has a rough upper limit of about 4%. For example, we have obtained that:

$$\frac{\eta_{\text{pipe}}}{\eta_{\text{bulk}}} = 0.96 \pm 0.15 \quad (1)$$

and similarly for the density.

### 9. Summarizing remarks

From the collection of qualitative observations reported above it comes out quite clearly that the falling of a heavy sphere (of whatever diameter) induces a modification of the viscous fluid along its path, resulting in the formation of a definite surface bounding the pipe. The appearance of such a surface is mainly responsible of the various mechanical and optical effects reported above; the physical properties of the liquid used themselves influence the dynamical evolution of the pipe and the geometrical properties of the pipe. The development of the phenomenon observed is certainly related to relaxation processes taking place in the viscous liquids employed (see, e.g., the point F2), but these “standard” processes appear to be not the main source of the phenomenon itself. Secondary effects, as those mentioned above, may easily hide the primary phenomenon concerning the “true” dynamics of the pipe, so that we have taken particularly care of avoiding such spurious effects (whenever possible) in our experimental measurements.

$x_{\text{glycerol}} = 0.99$			
	$d_0$	$t_0$ (min)	$\tau$ (min)
Phase 1	$0.202 \pm 0.005$	$-0.8 \pm 0.3$	$0.8 \pm 0.2$
Phase 2	$0.174 \pm 0.001$	$0.8 \pm 0.5$	$1.9 \pm 0.3$
Phase 3	$0.150 \pm 0.009$	$1 \pm 8$	$8 \pm 6$
Phase 4	$0.126 \pm 0.006$	$19 \pm 5$	$8 \pm 5$

$x_{\text{glycerol}} = 0.98$			
	$d_0$	$t_0$ (min)	$\tau$ (min)
Phase 1			
Phase 2	$0.155 \pm 0.003$	$-0.4 \pm 0.1$	$0.9 \pm 0.1$
Phase 3	$0.1398 \pm 0.0003$	$4.7 \pm 0.4$	$1.4 \pm 0.2$
Phase 4	$0.128 \pm 0.001$	$14 \pm 6$	$2 \pm 2$

$x_{\text{glycerol}} = 0.97$			
	$d_0$	$t_0$ (min)	$\tau$ (min)
Phase 1			
Phase 2			
Phase 3	$0.144 \pm 0.002$	$0.23 \pm 0.07$	$0.61 \pm 0.9$
Phase 4	$0.11 \pm 0.01$	$6 \pm 5$	$8 \pm 6$

$x_{\text{glycerol}} = 0.96$			
	$d_0$	$t_0$ (min)	$\tau$ (min)
Phase 1			
Phase 2	$0.17 \pm 0.01$	$-1.1 \pm 0.9$	$0.9 \pm 0.7$
Phase 3	$0.1219 \pm 0.0007$	$1.0 \pm 0.1$	$2.2 \pm 0.1$
Phase 4	$0.112 \pm 0.004$	$0.3 \pm 8.9$	$4 \pm 4$

$x_{\text{glycerol}} = 0.95$			
	$d_0$	$t_0$ (min)	$\tau$ (min)
Phase 1			
Phase 2	$0.172 \pm 0.001$	$0.4 \pm 0.1$	$0.9 \pm 0.1$
Phase 3	$0.15 \pm 0.01$	$1 \pm 3$	$2 \pm 2$
Phase 4	$0.129 \pm 0.002$	$3 \pm 2$	$4 \pm 1$

TABLE II: Fitting parameters for the extinction rates in Eq. (2) (see the text).

## B. Quantitative observations

### 1. Extinction rates of the pipe

Measurements of the diameter of the pipe divided by that of the falling sphere ( $d_{\text{ratio}} = d_{\text{pipe}}/d_{\text{sphere}}$ ) at given instants of time since pipe formation (chosen as the reference time  $t = 0$ ) have been performed as a function of the concentration of glycerol/water mixtures. Such observations have been carried out by illuminating the sample with normal (non laser) light and measuring the size of the shadow of the pipe and the sphere projected laterally on a screen. The given measurement ended when an appreciable shadow (with respect to the bulk liquid) was no more projected on the screen; note, however, that at this time the pipe continued to persist, as it has been observed by looking directly at the pipe from its top (see the point O1). The following measurements have been performed with spheres of diameter 5 mm, at a temperature of  $24 \div 25^\circ\text{C}$ .

R1. The time evolution of the pipe radius has always

$x_{\text{glycerol}} = 0.94$			
	$d_0$	$t_0$ (min)	$\tau$ (min)
Phase 1			
Phase 2			
Phase 3	$0.156 \pm 0.003$	$0.4 \pm 0.4$	$2.8 \pm 0.5$
Phase 4	$0.1465 \pm 0.0002$	$6.7 \pm 0.3$	$2.2 \pm 0.1$

$x_{\text{glycerol}} = 0.93$			
	$d_0$	$t_0$ (min)	$\tau$ (min)
Phase 1			
Phase 2			
Phase 3	$0.149 \pm 0.005$	$0.9 \pm 0.4$	$2.3 \pm 0.5$
Phase 4	$0.111 \pm 0.003$	$6.4 \pm 0.9$	$4 \pm 1$

$x_{\text{glycerol}} = 0.92$			
	$d_0$	$t_0$ (min)	$\tau$ (min)
Phase 1			
Phase 2			
Phase 3	$0.149 \pm 0.004$	$1.3 \pm 0.2$	$2.9 \pm 0.2$
Phase 4	$0.106 \pm 0.005$	$11.2 \pm 0.8$	$5 \pm 1$

$x_{\text{glycerol}} = 0.91$			
	$d_0$	$t_0$ (min)	$\tau$ (min)
Phase 1			
Phase 2			
Phase 3	$0.1105 \pm 0.0008$	$1.06 \pm 0.03$	$0.97 \pm 0.05$
Phase 4			

$x_{\text{glycerol}} = 0.90$			
	$d_0$	$t_0$ (min)	$\tau$ (min)
Phase 1			
Phase 2			
Phase 3			
Phase 4	$0.108 \pm 0.003$	$1.48 \pm 0.09$	$0.9 \pm 0.2$

TABLE II: Fitting parameters for the extinction rates in Eq. (2) (cont.).

an exponentially decreasing behavior (in given regions of time), for any concentration of the glycerol/water mixture. The fitting function employed with the set of measurements obtained is the following:

$$d_{\text{ratio}} = d_0 \left( e^{-\frac{t-t_0}{\tau}} + 1 \right). \quad (2)$$

The values of the fitting parameters are reported in Table II; note that the assignment of a certain parameter to a given “phase” (see the point R2) is somewhat arbitrary, and (partially) justified only *a posteriori*, by comparing the different values for different concentrations (and also introducing some theoretical bias; see Section III). In Fig. 6 we show the experimental data together with the fitting curve from Eq. (2).

The experimental points refer to averages over several sets of measurements, performed at given concentrations; the big error bars occurring in some cases are due to the (relatively) big deviation between these sets of data. Although the fitting procedures have been carried out on the average values obtained, we have always complied with the general information contained in *each* set of data

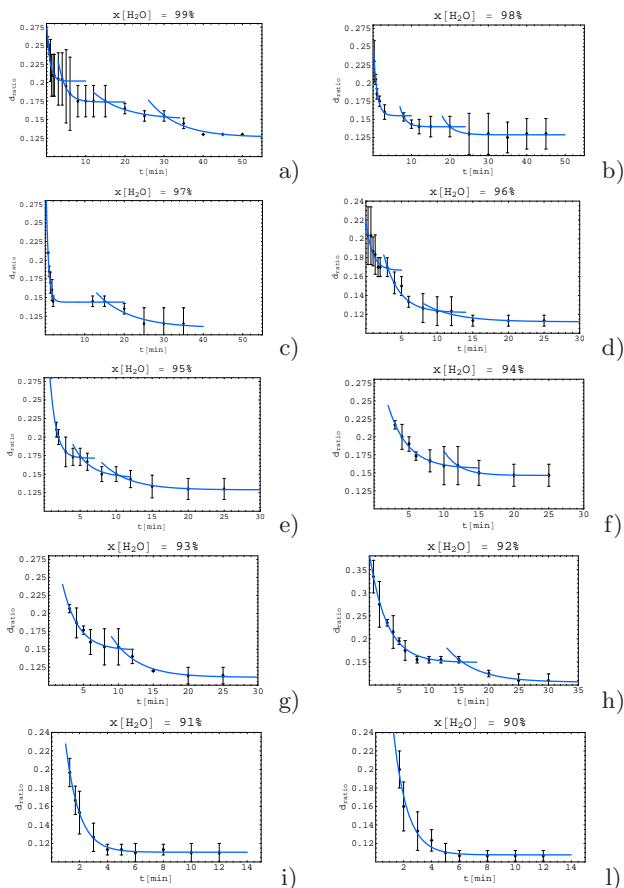


FIG. 6: Time evolution of the pipe radius for different water contents of the glycerol/water mixture (see the text).

and agreeing among those pieces of information. Thus, for example, although the big errors apparently do not support completely the adoption of a given fitting function rather than another, such adoption comes out, instead, from the statistical analysis of single sets of data. The same reasoning applies to the choice of the starting and the ending of the different fitting regions: the experimental data in two (or more) adjacent regions that, looking at average values, may be fitted by a single function within the errors, have been described by two (or more) different fitting curves, in agreement with what shown by any of the single sets of data conveying in the showed average values.

R2. The dynamical evolution of the pipe generated in glycerol/water mixtures takes place in different, subsequent time phases, each one characterized by its own exponential behavior. The trigger of such phases depends on the concentration of the mixture; the trigger times of the different phases (roughly, the intersection points of the different exponential curves, for given concentration) are reported in Table III.

## 2. Persistence time of the pipe

The persistence time  $t_{\text{persist}}$  of the pipe is defined as the time occurred since pipe formation till its visible disappearance, that is, till the intensity of the light reflected by the pipe and revealed from the top (parallel to the pipe axis) reduces below a given experimental threshold. We have performed a number of different runs aimed at measuring this quantity for pipes generated in different liquids, as function of key parameters (concentration and temperature), the results obtained being reported and discussed below.

R3. The pipe persistence time broadly decreases with decreasing glycerol concentration in glycerol mixtures reaching, however, two relative maxima for values of the concentration approximately given by:

$$x_{\text{glycerol}} \simeq 0.92, \quad x_{\text{glycerol}} \simeq 0.94 \quad (3)$$

for glycerol/water and:

$$x_{\text{glycerol}} \simeq 0.93, \quad x_{\text{glycerol}} \simeq 0.95 \quad (4)$$

for glycerol/ethanol mixtures, respectively. The experimental points are reported in Fig. 7 (we have used 3 mm spheres, at a temperature of 24°C and 24.5°C for glycerol/water and glycerol/ethanol mixtures, respectively).

R4. In the evolution dynamics of the pipe formed in glycerol/water and glycerol/ethanol mixtures, three different contributions have been found in the  $t_{\text{persist}}(x_{\text{glycerol}})$  plot; they are quite well described by gaussian fitting curves (see Fig. 8):

$$t_{\text{persist}} = t_a e^{-\frac{(x_{\text{glycerol}} - x_0)^2}{x_\sigma^2}} + t_b, \quad (5)$$

where the fitting parameters are reported in Table IV. Note that, in the region of greater concentration (case 1), the parameter  $x_0$  has been fixed to the maximum content of glycerol in the mixture. Instead, in the intermediate region of concentration (case 2), at least for glycerol/water mixtures, the reported values of the fitting parameters are purely indicative, since the small extension of the probed region does not allow an accurate determination of the parameters of the gaussian curve (near its maximum).

R5. The different contributions in the evolution dynamics of the pipe (see the point R4) do not manifest only at later times, in the persistence time curves, but are *independently* confirmed by the evolution curves of the pipe diameter at different times since formation, as showed in Fig. 9.

R6. The pipe persistence time (in pure glycerol) decreases with increasing temperature, according to three different behaviors (see Fig. 10a).

R7. In the evolution dynamics of the pipe generated in pure glycerol, different contributions have been found in the  $t_{\text{persist}}(T)$  plot; in the temperature regions where



	$t_{1 \rightarrow 2}$ (min)	$t_{2 \rightarrow 3}$ (min)	$t_{3 \rightarrow 4}$ (min)
$x_{\text{glycerol}} = 0.99$	4.2	15.5	30.6
$x_{\text{glycerol}} = 0.98$		7.8	20.0
$x_{\text{glycerol}} = 0.97$			15.6
$x_{\text{glycerol}} = 0.96$		3.1	10.4
$x_{\text{glycerol}} = 0.95$		5.2	10.5
$x_{\text{glycerol}} = 0.94$			12.3
$x_{\text{glycerol}} = 0.93$			10.3
$x_{\text{glycerol}} = 0.92$			15.5
$x_{\text{glycerol}} = 0.91$			–
$x_{\text{glycerol}} = 0.90$			–

TABLE III: Trigger times for the different exponential phases in the dynamical evolution of the pipe generated in different glycerol/water mixtures.

enough data are available, they are quite well described by gaussian fitting curves (see Fig. 10b):

$$t_{\text{persist}} = t_c e^{-\frac{(T-T_0)^2}{T_\sigma^2}}, \quad (6)$$

where the fitting parameters are reported in Table V.

R8. The curves  $t_{\text{persist}}(x_{\text{glycerol}})$  and  $t_{\text{persist}}(T)$ , obtained with evidently different experimental methods, may be compared when one assumes that the glycerol concentration and temperature variations contribute essentially to change only the viscosity  $\eta$  of the liquid. In such an assumption, by using known data on the dependence of  $\eta$  on the concentration and temperature of the mixtures [7], the  $t_{\text{persist}}(\eta)$  curves reported in Fig. 11 are obtained. From these curves it is evident that the appearance of different contributions to the evolution dynamics of the pipe is effectively ruled by the viscosity parameter, though a non negligible role is nevertheless played directly by the water (or ethanol) content of the mixture (through the concentration  $x_{\text{glycerol}}$ ) and by the thermal agitation (through the temperature  $T$ ) for viscosity values lower than approximately 550 mPa · s.

R9. The comparison of the persistence time curves for pipes generated in different viscous liquids reveals a similar behavior for the phenomenon studied which, however, develops on different time scales, as shown in Fig. 7. Note that the (extrapolated) matching at  $x_{\text{glycerol}} = 1$  of the curves, corresponding to glycerol/water and glycerol/ethanol mixtures, is not smooth.

R10. The persistence time of pipes generated in pure glycerol increases exponentially with the diameter of the generating sphere, as shown in Fig. 12. The fitting function appearing in this plot is:

$$t_{\text{persist}} = t_d \left( 1 - e^{-\frac{d_{\text{sphere}}}{D}} \right), \quad (7)$$

where  $t_d = 240 \pm 10$  min and  $D = 5.0 \pm 0.5$  mm.

Glycerol/water mixture				
	$t_a$ (min)	$t_b$ (min)	$x_0$	$10^4 x_\sigma^2$
1.	$110 \pm 6$	$31 \pm 6$	1	$8 \pm 1$
2.	17	27	0.941	1.0
3.	$25 \pm 3$	$9 \pm 2$	$0.922 \pm 0.003$	$8 \pm 4$
Glycerol/ethanol mixture				
	$t_a$ (min)	$t_b$ (min)	$x_0$	$10^4 x_\sigma^2$
1.	$68 \pm 2$	$11 \pm 3$	1	$9 \pm 1$
2.	$17 \pm 4$	$1 \pm 4$	$0.929 \pm 0.002$	$7 \pm 4$
3.	$6 \pm 2$	$19 \pm 2$	$0.950 \pm 0.001$	$0.5 \pm 0.4$

TABLE IV: Fitting parameters for the persistence time curves in Eq. (5) (see the text).

### 3. Summarizing remarks

The evolution dynamics of the pipes generated in viscous liquids comes out to be quite similar for different substances, but takes place on peculiar time scales and tends to be very fast for not high values of the viscosity, so that for moderately viscous or inviscid liquids the effect is practically unobservable.

The phenomenon appears to be completely settled by the liquid viscosity for  $\eta \geq 550$  mPa · s, and, in this region, the persistence time increases monotonically with increasing viscosity. Instead, for lower values of the viscosity, the microscopic structure of the liquid and its thermal energy play a non-negligible role: different contributions to the evolution dynamics come out at any instant of time since pipe formation, and the persistence time curves exhibit two maxima for peculiar values of the concentration (depending on the type of mixture used). In any of these regions, the persistence time curves are quite well approximated by gaussian fits, irrespective of the particular liquid mixture employed. It is particularly remarkable the fact that the appearance of such diverse contributions is confirmed by four independent observations (measurements of: persistence time vs glycerol/water concentration, persistence time vs glycerol/ethanol concentration, extinction rates at different times vs glycerol/water concentration and persistence time vs temperature).

The extinction rates of the pipes are always exponentially decreasing with time elapsed since formation, but different time scales for the evolution of the phenomenon have been observed, the appearance of which depends on the concentration of the liquid used.

## III. THEORETICAL INSIGHT

Our experimental analysis has shown a very rich phenomenology for the pipe effect, that cannot be simply accounted for standard relaxation effects. Although spurious effects, such as the dissolution of small air bubbles in the liquid, are sometimes present, we have seen that the primary phenomenon of the formation of a well-defined structure is not at all related to those secondary

	$t_c$ (min)	$T_0$ ( $^{\circ}\text{C}$ )	$T_{\sigma}^2$ ( $^{\circ}\text{C}^2$ )
1.	$11.0 \pm 0.2$	$36.0 \pm 0.3$	$49 \pm 8$
2.	$157 \pm 2$	$19.6 \pm 0.3$	$90 \pm 5$

TABLE V: Fitting parameters for the persistence time curves in Eq. (6) (see the text).

effects. Also, the possible dissolution of microscopic air bubbles located in the interstices of the surface of the metal sphere (these bubbles cannot be resolved with our experimental apparatus), as the explanation for the alteration of the properties of the liquid encountered by the falling body, is largely excluded by the size of the pipe formed and by the non-trivial phenomenology observed. Then, we have to search for a more complex theoretical explanation.

As a first step in the understanding of the phenomena reported above, let us assume that the falling of an heavy sphere in glycerol or other viscous media induces, substantially, only the formation of a *separation surface* between the bulk liquid and that in direct contact with the falling body. Possible slight alteration of the liquid properties, as effectively observed, will be not primarily taken into account for the moment.

Two main processes should, then, receive at least a rough explanation: the formation of such a surface and the time evolution of the pipe. These two items will be considered in the next paragraphs in the most simple way, leaving details (even important) for possible future studies.

### A. A microscopic model for pipe formation

The development of a surface in polar liquids, such as water, glycerol, etc., is characterized by a well definite orientation of the molecular dipole moments on the said surface [9] [10] [11]: the degree of polarization of the surface molecules is, effectively, greater than that of bulk ones. On the surface of the liquid, a net polarization of the molecular dipole moments develops, with an associated generation of a non-vanishing surface electric field and potential. Such polarization is, evidently, due to the presence of a polarizing electric field that for water, for example, derives from the non-vanishing permanent quadrupole moment of the water molecule. The polarizing electric field generates a torque on the surface molecules that tends to orientate the dipole moments along a given direction but, of course, a transition zone (that can extends even over  $10 \div 100$  molecular layers) exists before reaching the true bulk. More specifically, in liquids characterized by the presence of hydrogen bonds, domains can form where the dipoles are oriented along the direction of maximum polarization for the given domain, while the direction of maximum polarization of neighboring domains tend to rotate of  $180^{\circ}$  with respect to the previous one (similarly to the jux-

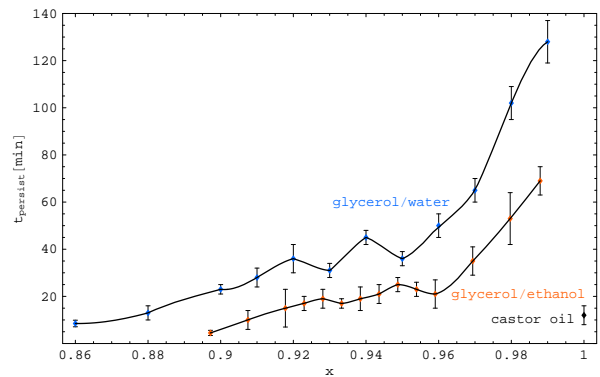


FIG. 7: Persistence time of pipes formed in glycerol/water ( $24^{\circ}\text{C}$ ) and glycerol/ethanol ( $24.5^{\circ}\text{C}$ ) mixtures as function of the glycerol concentration. For reference, the experimental point for the persistence time in pure castor oil ( $23^{\circ}\text{C}$ ) is reported as well (the dependence on the concentration for castor oil mixtures is practically unobservable with the presently adopted apparatus, due to the extremely low value of the persistence time).

taposition of north and south poles for magnets). The presence of an electric field, then, increases the number of “favorably” oriented domains at the expenses of the those less “favorably” ones, until a stationary state is reached.

Here we assume that the development of the pipe surface occurs in a way similar to the standard one described above. Very simply, the polarizing electric field may be thought as generated by the “friction” between the falling sphere and the viscid liquid, whose value is completely non-negligible due to the high viscosity of the liquids studied. An estimate of the order of magnitude for the field generated in such a way may be roughly obtained as follows.

The energy available from the falling sphere is that of the gravitational field, accounting for[17]:

$$U_G = m_{\text{sphere}} g h \simeq 3 \times 10^{-5} \text{J}. \quad (8)$$

A part of such energy will be dissipated in the production of heat (that is, it will increase just the thermal agitation of the liquid) due to the slowing down action of the liquid on the falling sphere. This energy may be calculated as the work  $U_S$  done by the Stokes force  $F = 6\pi R\eta v$  during the falling:

$$U_S \simeq 6\pi R\eta v_L^2 \vartheta \simeq 5 \times 10^{-6} \text{J} \quad (9)$$

[where  $v_L = 2(\rho_{\text{sphere}} - \rho_{\text{liquid}})gR^2/9\eta$  is the terminal velocity and  $\vartheta = 2\rho_{\text{sphere}}R^2/9\eta$  is the time constant of the instantaneous velocity of the sphere].

We assume that a non-vanishing energy  $U_P$  available for the polarization mechanism described above exists, whose order of magnitude is given by:

$$U_P \simeq U_G - U_S \approx 10^{-5} \text{J}. \quad (10)$$

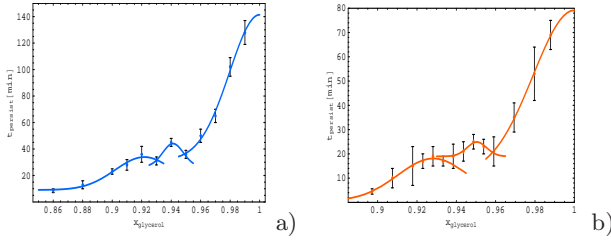


FIG. 8: Measured persistence times for pipes generated in glycerol water (a) and glycerol/ethanol (b) mixtures as functions of the glycerol concentration have been fitted by three different gaussian curves (see the text).

Such energy will be used to orientate the molecular electric dipoles, so that it will be proportional to the polarizing field  $E$ :

$$U_D = n \mu E, \quad (11)$$

where  $\mu$  is the electric dipole moment of the glycerol molecule and  $n$  the number of electric dipoles, which is *approximately* given by the number of molecules intercepted by the falling sphere. The number of molecules in 1 g of glycerol is  $n_0 = N_A/M \simeq 6.5 \times 10^{21}/\text{g}$  ( $N_A$  is the Avogadro number, while  $M$  the molecular weight of glycerol). For simplicity we assume that the pipe formed is a cylinder, so that  $m_{\text{pipe}} = \rho_{\text{liquid}} \pi R^2 h \simeq 0.4\text{g}$  and  $n = n_0 m_{\text{pipe}} \simeq 2.5 \times 10^{21}$  molecules. By equating Eq. (10) to Eq. (11) and using the values in Table I, we finally get:

$$E \approx 450 \text{ V/m}, \quad (12)$$

which is a fairly optimistic estimate, since  $U_G - U_S$  may be even lower by one order of magnitude (if the falling time is much greater than the time constant  $\vartheta$ ). Anyway, such an estimate completely agrees with the order of magnitude of the classic Frenkel estimate [12] of the surface potential of water, so that it is quite useful, in the following, to explore further the approximate microscopic model envisaged above.

In such scenario, it is very likely that the liquid molecules in the pipe and in the bulk near it experience a non-homogeneous electric field whose maximum amplitude is reached just on the pipe surface. It expectedly decreases away from the surface inside the pipe, while the field is practically zero in the bulk, where the “friction” action by the sphere is absent.

A non-homogeneous electric field  $\mathbf{E}$  exerts a translational force  $\mathbf{F}$  on a given molecule,

$$\mathbf{F} = (\boldsymbol{\mu} \cdot \nabla) \mathbf{E} + \alpha (\mathbf{E} \cdot \nabla) \mathbf{E} \quad (13)$$

( $\boldsymbol{\mu}$  and  $\alpha$  being the electric dipole moment vector and the polarizability of the liquid molecule, respectively), so that the molecules with a dipole moment pointing along the direction of  $\mathbf{E}$  will be pushed towards the regions with a greater field intensity. In such a way, a concentration gradient generates which induces a decrease of the density inside the pipe, with an effect similar to that of

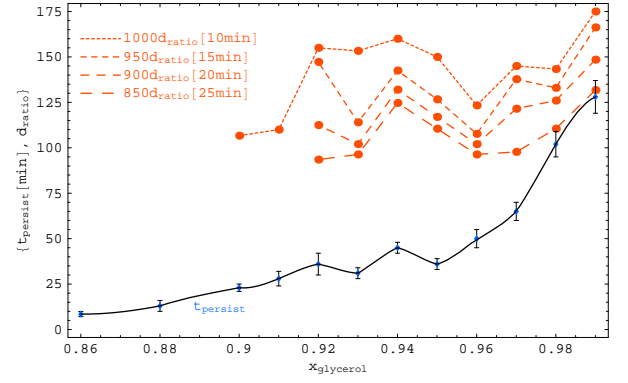


FIG. 9: Comparison between the persistence time curve (for pipes generated in glycerol/water mixtures) and the pipe diameters curves at subsequent time instants since formation, as a function of the glycerol concentration. The quantities  $d_{\text{ratio}}$  have been multiplied by a suitable rescaling factor (reported in the plot), in order to be easily recognizable, while arbitrary units have been adopted on the vertical axis.

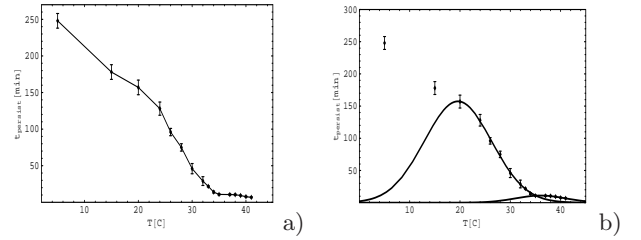


FIG. 10: Persistence time for pipes generated in pure glycerol as function of the temperature: a) interpolation of the experimental points; b) data fitting with two different gaussian curves.

electrostriction. From the standard theory of such effect [10] we can evaluate the variation  $\Delta\rho = \rho_{\text{bulk}} - \rho_{\text{pipe}}$  of the density between the pipe and the bulk, obtaining:

$$\frac{\Delta\rho}{\rho_{\text{bulk}}} \simeq \frac{E^2}{8\pi} \beta \rho_{\text{bulk}} \left( \frac{\partial \varepsilon}{\partial \rho} \right)_T \equiv \left( \frac{E}{E_0} \right)^2, \quad (14)$$

where  $\beta$  and  $\varepsilon$  are the isothermal compressibility and dielectric constant of the (bulk) liquid. As a simplifying assumption, we take valid [10] the Debye theory of electric polarization for calculating the variation of the dielectric constant with the density,

$$\left( \frac{\partial \varepsilon}{\partial \rho} \right)_T \simeq \frac{3}{M} \frac{\varepsilon - 1}{\varepsilon + 2}. \quad (15)$$

From the values in Table I we get the following estimate for the typical field  $E_0$  defined in Eq. (14):

$$E_0 \approx 260 \text{ V/m}, \quad (16)$$

which is of the same order of magnitude of the field in Eq. (12).

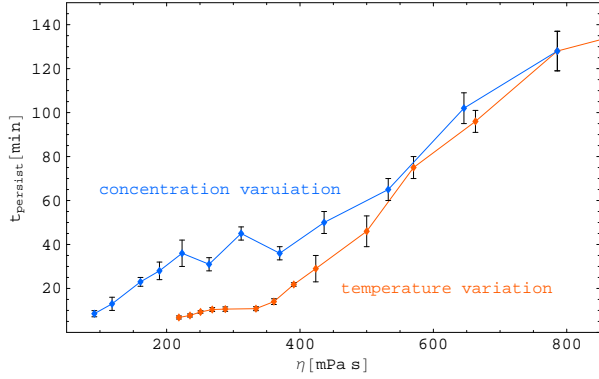


FIG. 11: Persistence time curves, for pipes generated in glycerol/water mixtures, as functions of the viscosity. The variation of the viscosity has been induced in two different ways: by varying the glycerol concentration (upper curve) or the temperature (lower curve) of the mixture.

By assuming, as suggested by the preliminary experimental data (1), that

$$\frac{\Delta\rho}{\rho_{\text{bulk}}} \approx \frac{\Delta\eta}{\eta_{\text{bulk}}} \simeq 4 \times 10^{-2},$$

we deduce that the electric field required to generate such a variation of the density, according to the mechanism described, would be:

$$E \approx 0.2E_0 \approx 50 \text{ V/m}, \quad (17)$$

an order of magnitude estimate in evident agreement with the independent one obtained above in Eq. (12).

A slight increase of the liquid density near the pipe surface, with an associated decrease inside the pipe, due to presence of the polarizing electric field, implies a corresponding change  $\Delta\varepsilon$  of the dielectric constant of the liquid in the pipe with respect to the bulk, as anticipated by the formulae above. From the standard theory [10] we have:

$$\Delta\varepsilon \simeq \frac{E^2}{4\pi} \beta \rho_{\text{bulk}}^2 \left( \frac{\partial\varepsilon}{\partial\rho} \right)_T \simeq \frac{6}{M} \frac{\varepsilon - 1}{\varepsilon + 2} \left( \frac{E}{E_0} \right)^2 \quad (18)$$

(within the mentioned approximations). For  $(E/E_0)^2 = \Delta\rho/\rho_{\text{bulk}} \simeq 4 \times 10^{-2}$  we get:

$$\Delta\varepsilon \approx 2 \times 10^{-3}. \quad (19)$$

The variation of the dielectric constant between the pipe and the bulk is, thus, negligible, so that the optical properties of the pipe are practically equal to those of the bulk. This, however, does not apply to the interface, i.e. on the pipe surface, where a gathering of electric dipoles is present. In all respects, the pipe behaves as a (almost cylindrical) dielectric shell, as indeed observed experimentally.

## B. A thermodynamical model for pipe evolution

Once the surface of the pipe has been formed by the falling of a sphere, the subsequent evolution consists just in the thinning of the pipe itself. More precisely, according to our observations (see the points E2-E3), we may distinguish the main, most relevant, process of pipe narrowing followed by a final “dissolution” of the pipe, which gets deformed. In the narrowing process the pipe keeps its structure, while it “dissolves” once the pipe radius reduces to small fractions of its initial value. Here we focus our attention on the main narrowing process, which we will show it can be described by standard thermodynamical procedures.

As a starting point, we assume that the narrowing process takes place at approximately constant pressure (that of the bulk liquid) and that no appreciable heat transfer occurs with the surroundings. In other words, the bulk liquid is thought as a pressure reservoir, inside which the narrowing of the pipe occurs adiabatically. In such approximations, the work made to narrow the pipe is stored as enthalpy of the system: the change of enthalpy  $dH$  for an almost isobaric, adiabatic change of state is the utilizable work  $dW$  gained by the system aside from the volume work [13]. This is essentially the work done by the liquid to induce a variation  $dA$  of the pipe surface, which is equal to  $\sigma dA$  ( $\sigma$  being the surface tension of the viscous liquid, whose value is supposed to be equal in the bulk and in the pipe). As a simplifying assumption, we will also consider that the internal energy of the pipe does not change while it evolves, so that the change of enthalpy is given by  $PdV + VdP$ ,  $V$  being the pipe volume and  $P \equiv P_{\text{bulk}} - P_{\text{pipe}}$  the net pressure. The condition above reads, then:

$$PdV + VdP \simeq \sigma dA. \quad (20)$$

The interpretation of such equation is straightforward: the energy spent in reducing the pipe surface ( $\sigma dA$ ) equals the work done in reducing the pipe volume ( $PdV$ ) plus the energy to contrast the variation of the bulk reservoir ( $VdP$ ), similarly to what happens in the classical Joule-Thomson effect (where, however, no surface variation occurs, so that  $dH = 0$ ). For simplicity we consider the pipe as a cylinder of radius  $r$  and height  $h$  much greater than the radius, so that  $dV = 2\pi h r dr$  and  $dA \simeq 2\pi h dr$ . By substituting in Eq. (20), we have:

$$r^2 \frac{dP}{dr} + 2(rP - \sigma) = 0. \quad (21)$$

The solution of this differential equation[18] is the following:

$$P = \frac{2\sigma}{r} \left( 1 \pm \frac{r_0}{r} \right), \quad (22)$$

where  $r_0$  is a (positive) integration constant with the dimensions of a length. As shown in Fig. 13, the solution  $P(r)$  depends crucially on the sign above; if the negative

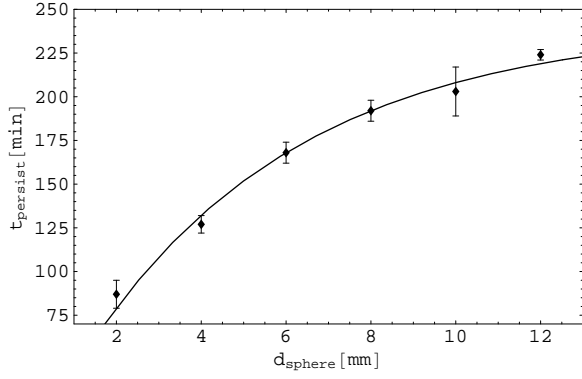


FIG. 12: Persistence time of pipes generated in pure glycerol ( $24.5 \div 25^\circ\text{C}$ ) as a function of the diameter of the generating spheres.

sign is taken,  $P(r)$  has a relative maximum and goes to zero for  $r = r_0$ .

From the physical viewpoint, some considerations are in order. If the positive sign is considered in Eq. (22), the difference  $P_{\text{bulk}} - P_{\text{pipe}}$  is positive for any radius of the pipe, and indefinitely increases for  $r$  approaching zero. Then, in such a case, the pipe expands, this situation not corresponding to what observed. Instead, If the negative sign is taken in Eq. (22), the difference  $P_{\text{bulk}} - P_{\text{pipe}}$  is positive for large radii and increases till a maximum; after that, the net pressure decreases, reaching the equilibrium condition  $P_{\text{bulk}} = P_{\text{pipe}}$  for  $r = r_0$ , and becomes indefinitely negative for  $r$  approaching zero. Actually, the narrowing of the pipe corresponds to the last case, when its radius decreases from the maximum value  $2r_0$  to the value  $r_0$ .

We can then envisage the following picture. At the very beginning, just after the falling of the sphere, when the pipe undergoes a rapid thinning (see the point D1), the surface “compresses” the liquid inside the pipe, inducing an increase of the internal pressure ( $P_{\text{pipe}}$ ) till a maximum  $P_{\text{max}} = \sigma/2r_0$  for  $r = 2r_0$ . By introducing the numerical values of Tables I and II, we have  $P_{\text{max}} \approx 300$  Pa, which is a reasonable small value (in the present model) for the pressure difference. This first region corresponds to the balance of the surface effects with the volume ones,  $\sigma dA = PdV$  (that is,  $VdP \simeq 0$ ), for which  $P \simeq \sigma/r$ . By decreasing the radius  $r$ , the volume effects become subdominant with respect to the surface ones, while the role of the energy contrasting the variation of the bulk reservoir is no more negligible. This continues until  $P_{\text{bulk}} = P_{\text{pipe}}$  for  $r = r_0$ , and such equilibrium point may be considered as “conclusive” of the narrowing process, since for  $r < r_0$  we have  $P_{\text{pipe}} > P_{\text{bulk}}$ .

The present model, then, predicts naturally the appearance of a length scale  $r_0$ , which can be directly related to the observed value  $d_0$  in Eq. (2). Indeed, on one hand,  $r = r_0$  is the value of the pipe radius at which the narrowing process “ends”; on the other hand,  $d_0 \cdot r_{\text{sphere}}$  (with  $d_0$  in Eq. (2)) is just the value of the pipe radius

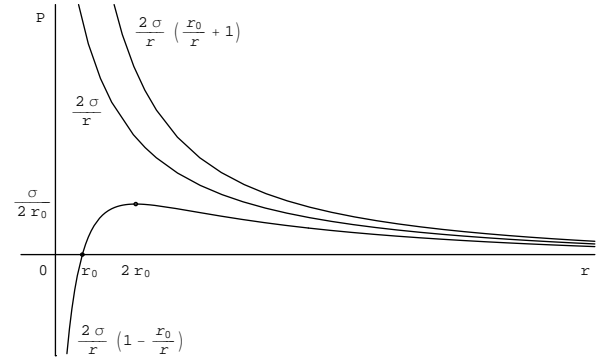


FIG. 13: The different solutions of Eq. (21) according to the values of the integration constant  $y_0$ .

for  $t \rightarrow +\infty$ , so that we simply have:

$$r_0 = d_0 \cdot r_{\text{sphere}}. \quad (23)$$

The phenomenological interpretation of the parameter  $t_0$ , that is the “initial” time [19] of the narrowing process, as deduced from experimental observations, is as well straightforward in the present model. In fact, from Eq. (2) it follows immediately that the time  $t_0$  corresponds to the point  $d_{\text{ratio}} = 2d_0$  and, from what said above, for  $r = 2r_0$  the net pressure  $P_{\text{bulk}} - P_{\text{pipe}}$  takes its maximum. We then have:

$$P|_{t=t_0} = P_{\text{max}} = \frac{\sigma}{2r_0} \quad (24)$$

The appearance of different phases in the time evolution of the pipe, as observed in Fig. 6 (see the point R2), may be described in the present scheme in terms of a sudden change of the net pressure. Indeed,  $r_0$  decreases from one phase to the following (see the values of  $d_0$  in Table II), so that from Eq. (24) an increase of  $P_{\text{max}}$  follows. The change of the time scale during the pipe evolution is, then, caused by an increase of the net pressure or, more specifically, by a decrease of the pipe pressure.

The evolution of  $P$  with time  $t$  may be obtained by inserting Eq. (2) into Eq. (22) (with the minus sign):

$$P = \frac{2\sigma}{r_0} \frac{e^{-\frac{t-t_0}{\tau}}}{\left(1 + e^{-\frac{t-t_0}{\tau}}\right)^2}. \quad (25)$$

The curve  $P(t)$  is, thus, symmetric with respect to  $t = t_0$ . Near its maximum, that is at the start of pipe narrowing, it is approximated by a gaussian centered around  $t_0$  and with full width at half maximum equal to  $2\tau$ :

$$P \simeq \frac{\sigma}{2r_0} e^{-\frac{(t-t_0)^2}{4\tau^2}}. \quad (26)$$

Instead, at the end of the narrowing (for  $r$  approaching  $r_0$ ), the net pressure decreases exponentially with a time constant  $\tau$ :

$$P \simeq \frac{2\sigma}{r_0} e^{-\frac{t-t_0}{\tau}}. \quad (27)$$



An increase of  $P$  from one phase to the following then corresponds to an increase of  $t_0$  and/or  $\tau$ , in agreement with the experimental data (see Table II).

Summing up, we find that pipe evolution is perceptible when  $P_{\max}$  is sensibly different from zero, that is for quite large values of  $\sigma$  and/or  $r_0$  as, indeed, effectively observed. In general, the effect studied is ruled *only* by these two parameters. We also point out that, in glycerol/water mixtures, an increase of the water content leads to an increase of the surface tension  $\sigma$ , so that we have an increase of  $P_{\max}$ . Since, according to Eq. (25), the difference between bulk and pipe pressure increases, the narrowing process is thus faster for water-rich mixtures, as it is generally apparent in Figs. 6 or 8. The interpretation of the maxima in Figs. 8, as well as other peculiar observations, is however beyond the range of the present thermodynamical model, and claims for a more detailed microscopic interpretation of the phenomenon.

#### IV. CONCLUSIONS

In this paper we have studied in detail the pipe effect occurring in viscous liquids which, despite its simplicity, at the best of our knowledge it has not been reported previously in the literature. The effect, observed here in pure glycerol, in glycerol/water and glycerol/ethanol mixtures, and in castor oil, consists in the formation of a well-defined structure (a pipe) after the passage of a heavy body in the viscous liquid, this structure lasting for quite a long period.

A very rich phenomenology has been observed for such effect, that cannot be trivially explained in terms of standard relaxation and/or spurious effects like the dissolution of air bubbles in the part of liquid encountered by the falling body.

A part of this phenomenology may be well summarized by simply admitting that the pipe effect is primarily due to the formation of a separation surface, upon which mechanical action of even different kind may be performed. The apparently non-obvious optical effects observed are, then, just the manifestation of this surface to light (normal or laser) impinging on it.

The time evolution of the present phenomenon is, as well, not at all trivial, as our quantitative measurements of the extinction rates and persistence time curves of the pipe have shown. While the pipe gets thinner and thinner as the time goes on, it experiences different exponentially decreasing time phases, with different time scales, this effect being likely due to sudden changes of the liquid pressure inside the pipe. By lowering the viscosity of the sample liquid, the persistence time of the pipe gets shorter, till quite a complete non-observability of the effect for not high values for the viscosity. This transition has been accurately studied by measuring the persistence time curves for glycerol/water (or glycerol/ethanol) mixtures with decreasing content of glycerol. As expected, the persistence time generally decreases with decreas-

ing concentration of glycerol but, quite interestingly, two maxima have been observed for given concentrations, this behavior being confirmed by several independent observations.

Our study has not been limited to experimental observations, but we have also tried to construct a theoretical model for the formation and the evolution of the pipe, able to interpret (at least a part of) the data found.

We have, thus, assumed that the falling body induces a non-negligible polarizing electric field in highly viscous liquids. It tends to orientate the molecular dipole moments of the liquid (the samples employed are highly polar liquids, with the presence of hydrogen bonds) in the neighborhood of the falling body surface, thus generating a dielectric shell (the separating liquid surface) that would be responsible of (part of) the phenomenology observed. Indeed, order of magnitude estimates of the polarizing electric field, for the case studied here, show that such picture could not be far from reality, since the model brings to definite predictions that have been effectively observed.

The dynamical evolution of the pipe, once formed according to the microscopic model proposed, seems, then, well described by a thorough thermodynamical model. According to this, the evolution is just the macroscopic result of the balance of two competing actions: the expansion of the pipe surface ruled by the surface tension effect, contrasted by the bulk liquid that is assumed to be an almost perfect pressure reservoir. This model gives a likely account of the experimentally observed appearance of a length scale  $r_0$  in the extinction rate of the pipe. Together with the surface tension parameter, it rules the behavior of the net pressure acting on the pipe surface, which reaches a maximum at the onset of the narrowing process, the “initial” time  $t_0$  being directly obtained from measurements. Several other predictions come out from the model studied, fitting quite well with the experimental observations.

Although some understanding of the effect observed has been apparently reached, it should be regarded mainly as preliminary, since further experimental investigations are needed. Also, the interpretative models proposed for the formation and evolution of the pipe should be considered, as well, just as a starting theoretical framework, which claims for a more detailed inspection. Novel results, from both theory and experiments, are then likely to be expected.

#### Acknowledgments

The present study was inspired by some observations from a student of one of us (S.E.), Riccardo Frasca; our gratitude to him and to Chiara Baldassarri for essential experimental assistance is here acknowledged. Moreover, it would not have been possible to carry out accurately

the experiments discussed in this paper without the valuable help of Ercole Gatti, Marco Marengo and his group

(Alfio Bisichini, Stefano dall'Olio, Carlo Antonini), Massimo Lorenzi, Giovanna Barigozzi and Giuseppe Rosace.

- 
- [1] P.K. Dixon, L. Wu and S.R. Nagel, *Phys. Rev. Lett.* **65** (1990) 1108; W. Götze and L. Sjögren, *Rep. Prog. Phys.* **55** (1992) 241; P. Lunkenheimer, A. Pimenov, M. Dressel, Yu.G. Goncharov, R. Böhmer and A. Loidl, *Phys. Rev. Lett.* **77** (1996) 318; C. Hansen, F. Stickel, T. Berger, R. Richert and E.W. Fischer, *J. Chem. Phys.* **107** (1997) 1086; C.A. Angell, K.L. Ngai, G.B. McKenna, P.F. McMillan and S.W. Martin, *J. Appl. Phys.* **88** (2000) 3113; S. Sudo, M. Shimomura, N. Shinyashiki and S. Yagihara, *J. Non-Cryst. Solids* **307 - 310** (2002) 356; Th. Blochowicz, Ch. Tschirwitz, St. Benkhof and E.A. Rössler, *J. Chem. Phys.* **118** (2003) 7544; A. Sanz, M. Jimenez-Ruiz, A. Nogales, D. Martín y Marero and T.A. Ezquerro, *Phys. Rev. Lett.* **93** (2004) 015503; Li-Min Wang, S. Shahriari and R. Richert, *J. Phys. Chem. B* **109** (2005) 23255.
- [2] E. Donth, *The Glass Transition: Relaxation Dynamics in Liquids and Disordered Materials* (Springer, Berlin, 2001); F. Kremer and A. Schönhals (Eds.), *Broadband Dielectric Spectroscopy*; (Springer, Berlin, 2003);
- [3] J.W. Lawrie, *Glycerol and the glycols: Production, properties and analyses* (Chemical Catalog Company, New York, 1928); C.S. Miner and N.N. Dalton, *Glycerol* (Reinhold, Baltimore, 1953); A.R. Ubbelohde, *The Molten state of matter* (Wiley, New York, 1978; Chap. 16).
- [4] R.E. Lee, Jr., C.P. Chen, and D.L. Denlinger, *Science* **238** (1987) 1415; F. Franks (Ed.), *Water: A comprehensive treatise* (Plenum, New York, 1982, Vol. 7).
- [5] P. Mazur, *Science* **168** (1970) 939; G.M. Fahy, D.I. Levy and S.E. Ali, *Cryobiology* **24** (1987) 196; Z. Chang and J.G. Baust, *ibid.* **28** (1991) 268; G. Vigier and R. Vassoille, *ibid.* **24** (1987) 345; P. Boutron and F. Arnaud, *ibid.* **21** (1984) 348.
- [6] C.A. Angell, in K.L. Ngai and G.B. Wright (Eds.), *Relaxations in complex systems* (NRL, Washington D.C., 1985); R. Böhmer and C.A. Angell, *Phys. Rev. B* **45** (1992) 10091.
- [7] See the websites:  
<http://www.dow.com/glycerine/resources/physicalprop.htm>,  
<http://www.thegoodscentscompany.com/data/rw1008461.html>,  
<http://en.wikipedia.org/wiki/Glycerol>.
- [8] See the website <http://www.lsbu.ac.uk/water/data.html> and references therein.
- [9] H. Eyring, D. Henderson and W. Jost (eds.), *Physical chemistry: An advanced treatise*, Vol. VIII A - Liquid state, edited by D. Henderson (Academic Press, New York, 1971).
- [10] C.J.F. Bottcher, *Theory of electric polarization* (Elsevier, Amsterdam, 1973)
- [11] C.A. Croxton, *Statistical mechanics of the liquid surface* (Wiley, New York, 1980).
- [12] J. Frenkel, *Kinetic theory of liquids* (Dover, New York, 1955).
- [13] L.E. Reichl, *A modern course in statistical physics* (Wiley, New York, 1998, 2nd edition), pp.40 ff.; W. Greiner, L. Neise and H. Stöcker, *Thermodynamics and statistical mechanics* (Springer, New York, 1995), pp.95 ff.
- [14] Note that even in glycerol/ethanol mixtures a small content of spurious water is present, not lower than 1%, mainly due to the content of water in the “pure” glycerol employed.
- [15] Illuminated by normal, not laser, light (see the point O4), the smaller pipe appears on a screen with a darker shadow with respect to that of the larger one, though always darker with respect to the bulk glycerol.
- [16] With an appropriate illumination with normal light.
- [17] Here and in the following, for our numerical estimates we use typical values as used in our experimental setup; for example we take spheres of radius  $R \approx 1$  mm falling in glycerol from an height of  $\approx 10$  cm, etc.
- [18] It may be easily obtained by the change of variable  $P \rightarrow y \equiv r^2 P / \sigma$  ( $y$  has the dimensions of a length).
- [19] Note that, according to observations, the present model would apply only to the “stationary” pipe evolution, while other effects occurring just at the formation of the pipe or soon after that are not included. Thus, it is practically meaningless to consider the part of the  $P(r)$  curve for  $r > 2r_0$ .